OBSERVATIONS AND MODEL OF SEDIMENT TRANSPORT NEAR THE TURBIDITY MAXIMUM OF THE UPPER ST. LAWRENCE ESTUARY

by

P.F. Hamblin

NWRI Contribution No. 88-42

Lakes Research Branch
National Water Research Institute
Canada Centre for Inland Waters
Burlington, Ontario, Canada L7R 4A6

August 1988

ABSTRACT

The need to investigate the role of suspended sediments in the transport and fate of chemical contaminants in the St. Lawrence Estuary has led to the measurement of profiles of suspended sediments, horizontal current, temperature and salinity at an anchor station approximately 60 km downstream from the turbidity maximum. Hourly profiles over nearly three semi-diurnal tidal cycles reveal peaks of suspended sediment concentration following maximum flood and ebb currents at the bottom, whereas near the surface there is only one maximum in suspended sediment concentrations per tidal cycle. Observations of the distributions of suspended sediment and its horizontal flux suggest that local resuspension is the controlling factor at the measurement site.

This study demonstrates that landward sediment flux in the lower layer is maintained by the ebb-flood asymmetry mechanism described by Dronkers (1986) and by the asymmetry in vertical mixing due to fluctuations in stratification related to the intrusion of the salt wedge. The latter mechanism is explored in detail by means of a vertical transport model for fine-grained newly deposited sediments. The model employing

standard prescriptions for mixing and resuspension results in the best match between simulated and observed sediment distributions for a particle sinking velocity of 3×10^{-4} m/s. This settling rate corresponds to a mean particle size of 15 μm which compares closely with the average observed particle size of 10 to 20 μm (Krank, 1979).

RÉSUMÉ

Pour étudier le rôle que jouent les sédiments en suspension dans le transport et le devenir des contaminants chimiques dans l'estuaire du Saint-Laurent, on a établi le profil des sédiments en suspension, des courants horizontaux, de la température et de la salinité dans une station d'observation située à quelque 60 km en aval du point de turbidité maximale. L'analyse de profils tracés toutes les heures pendant presque trois cycles tidaux semi-diurnes révèle que la concentration de sédiments en suspension au fond de l'eau monte en flèche à plusieurs reprises après les flux et les reflux maximaux, tandis que près de la surface, elle n'atteint un maximum qu'une fois par cycle tidal. D'après les données qu'on a pu recueillir sur la distribution et le flux horizontal des sédiments en suspension, le processus de remise en suspension local serait le facteur déterminant au point d'observation.

L'étude permet de démontrer que dans la couche la plus basse, le flux de sédiments vers les terres se maintient à cause du mécanisme d'asymétrie du flux et du reflux que décrit Dronkers (1986) et de l'asymétrie du mélange vertical résultant des fluctuations de stratification qu'entraîne la pénétration du coin salé. Ce dernier mécanisme peut s'étudier de façon approfondie au moyen d'un modèle de transport vertical s'appliquant aux

sédiments à grain fin de décantation récente. Dans ce modèle, les prescriptions standard relatives au mélange et à la remise en suspension sont telles que la concordance est maximale entre la distribution des sédiments simulée et observée lorsque la vitesse de sédimentation est de 3×10^{-4} m/s. Cette valeur s'applique à une particule de grosseur moyenne de 15 um, ce qui concorde bien avec la valeur moyenne observée qui est de 10 à 20 um (Krank, 1979).

MANAGEMENT PERSPECTIVE

The Upper Estuary of the St. Lawrence River is one of the most complex water bodies known due to its complicated bathymetry, strong tidal flows, turbulent mixing and sharp density fronts. The little-known sediment transport in this complex setting would be sufficient justification for study were it not for the crucial role played by suspended sediments in the partitioning between the dissolved and particulate phases of metal and organic contaminants. Public concern for possible contamination of the biota of the St. Lawrence Estuary, particularly the larger species such as eels and beluga whales, has motivated a study of the distribution and transport of trace metals and organic contaminants during the field season of 1986. Observations of the flow fields, salinity, and suspended sediments were made concurrently with the contaminant chemistry with the aim of providing information on the processes responsible for the distribution and transport of contaminants.

A simple one-dimensional vertical transport model of the suspended sediment fluctuations taken at an anchor station reproduced the main features of the observations and allowed the settling speed and average particle size to be deduced. Application of the model allows generalization of the observations that could be useful in determining the contaminant dynamics. The results also provide input into more refined field experiments and the development of more elaborate models.

PERSPECTIVE GESTION

La complexité de la bathymétrie du haut estuaire du fleuve Saint-Laurent, les courants de marée puissants, le mélange par turbulence et les fronts de densité marqués qui caractérisent cette étendue d'eau en font l'une des plus complexes que nous connaissions. Le fait que le transport des sédiments soit mal connu est déjà une raison suffisante dans ces conditions pour qu'on en entreprenne l'étude, mais la chose est d'autant plus justifiée que les sédiments en suspension jouent un rôle crucial dans la séparation des contaminants métalliques et organiques entre la phase dissoute et la phase en particules. La population s'inquiétant de la possibilité de la contamination du biote de l'estuaire du Saint-Laurent, en particulier de certaines espèces comme les anguilles et les baleines béluga, on a étudié la distribution et le transport des métaux présents à l'état de traces et des contaminants organiques durant la saison de travaux sur le terrain de 1986. En même temps qu'on recueillait des données sur les champs de courants, la salinité et les sédiments en suspension, on étudiait la chimie des contaminants afin de connaître les processus mis en jeu dans la distribution et le transport de ces derniers.

Au moyen d'un modèle simple unidimensionnel de transport vertical représentant les fluctuations des sédiments en suspension mesurées dans une station d'observation, on a reproduit les principales caractéristiques des phénomènes observés et l'on a pu déduire la vitesse de sédimentation et la grosseur moyenne des particules. Ce modèle permet de tirer des généralisations des observations qui peuvent servir à comprendre la dynamique des contaminants. Les résultats qu'on obtient servent aussi à la réalisation sur le terrain d'expériences plus raffinées et à l'élaboration de modèles plus perfectionnés.

Introduction

The Upper Estuary of the St. Lawrence River is one of the most complex water bodies known due to its complicated bathymetry, vigorous tidal currents and turbulent mixing and pronounced gradients in density both horizontally and vertically due to massive fresh water input. The limited knowledge of sediment transport in this complex setting would be sufficient justification for study were it not for the crucial role played by suspended sediments in the partitioning between the dissolved and particulate phases of metal and organic contaminants (Nichols, 1986). For example, in the St. Lawrence Estuary, Cossa and Poulet (1978) and Bewers and Yeats (1979) pointed out that a region of high suspended sediment concentrations known as the turbidity maximum has profound influence upon the distributions of total iron, manganese and cobalt through adsorption-desorption processes.

Public concern for possible contamination of the biota of the St. Lawrence Estuary, particularly the larger species such as eels and beluga whales has motivated a study of the distribution and transport of trace metals and organic contaminants during the field season of 1986. The observations discussed in the present paper were measured concurrently with the

contaminant chemistry with the aim of providing information on the processes responsible for the distribution and transport of such contaminants as cadmium, lead and volatile hydrocarbons in the St. Lawrence Estuary. In the following, a brief review of prior work in the estuary is restricted to suspended sediments and their transport. The reader is referred to El-Sahb (1988) for a review of the physical oceanography of the St. Lawrence Estuary.

The St. Lawrence Estuary is no exception to estuaries in general which exhibit zones of enhanced turbidity in the transition between river and sea water. Soucy et al. (1976) were the first to describe the turbidity zone of the St. Lawrence and relate it to such sedimentary processes as sediment flocculation and recycling due to the residual gravitational circulation. They found that augmented suspended sediment concentrations are more likely to be due to the estuarine circulation than flocculation and that much work needed to be done before a sediment transport model could be developed. d'Anglejan and Smith (1973) measured surface and bottom suspended sediments at several stations in the Upper Estuary and related them to vertical density differences over the tidal cycle. d'Anglejan and Ingram (1976) were the first to measure profiles of suspended sediment simultaneously with

current profiles and hence deduced the horizontal sediment transport. Unfortunately, their anchor stations were limited to the zone downstream of Pointe-au-Pic (Figure 1) and therefore not close to the turbidity maximum. They found that horizontal advection is more important than local resuspension over the tidal cycle in this deeper portion of the estuary and that concentrations of suspended sediments were maximum at mid-depth as opposed to near the bottom. Silverberg and Sundby (1979) studied the sediments of the entire system from the fresh water region at Quebec to open sea conditions by the Saguenay Fjord as well as the seaward response of the suspended sediment distributions to fluctuations in river discharge. An important contribution was the determination of particle size spectra for upper (fresh water), middle (turbidity maximum) and lower (seawater) reaches of the estuary. Particle sizes are more uniform or better sorted within the turbidity maximum or middle portion than at either end. Other findings were that local resuspension as opposed to horizontal transport was an important factor in suspended sediment distribution in the shallower upper reaches and that maximum turbidities occurred just after the start of the flood tide. No current measurements were taken in their study.

In a further elaboration of the particle size distribution in the Upper Estuary, Krank (1979) found that in the turbidity maximum the most frequent particle size remained in the range 10-20 μm over the tidal cycle both at the surface and bottom although the concentrations changed dramatically. She pointed out that the turbidity maximum is maintained, in part, by tidal current asymmetry which was inferred at one station where she noted that the peak bottom speed was greater during flood than during ebb conditions. d'Anglejan (1981) has reviewed the work on the suspended sediment dynamics of the Upper Estuary up to the late 1970's.

In a recent study of high frequency suspended sediment concentrations and sediment flux, d'Anglejan and Ingram (1984) measured bottom concentrations and currents over long periods with moored instrumentation. They were able to show that seasonal trends in sediment concentration related to the freshwater discharge and the necessity for high frequency sampling of suspended material with their rapid response sensor.

In the present study those measurements that suggest the formulation of a simple one-dimensional model of the vertical transport of suspended sediment are first discussed. The

model results are then compared to the field observations in order to determine a key unspecified model parameter. Finally, the calibrated model is applied to the problem of maintenance of the turbidity maximum and the associated contaminant fluxes.

Methods

A series of four anchor stations from Quebec to the Saguenay River were occupied for periods of a day or longer from June to July 1986 (Figure 1). At all stations, suspended sediment concentrations were measured by centrifuging over 100 minutes 600 L of water drawn at the depths of either 3 or approximately 12 m. When suspended sediment concentrations were not too high profiles of optical transmission were recorded hourly by a profiling transmissometer of 25 cm path-length. Optical transmission was related to sediment concentrations at the continuous sampling depth. Vertical profiles of salinity were measured with an Applied Microsystems CTD and current speed, direction and temperature by a Neil Brown direct reading acoustic current meter. Field calibrations of the transmissometer and laboratory calibrations of the acoustic current meter prior to field deployment are given in Hamblin (1986) as

well as the method for computing the tidally averaged flow from time series. Special attention was given to eliminate magnetic field disturbances by the hull of the research vessel on the magnetometer aboard the current meter.

Observations

During the field experiment river discharges were estimated to be from 12 to 13 (10^3 m^3/s) and tides were either at near neap or neap phases. At station 253 the salinity is not appreciably different from the upper reaches of the St. Lawrence River and suspended sediments range from concentrations of 8 mg/L to 16 mg/L which agree with Silverberg and Sundby (1979). At the seaward extent, station 6E400, the salinity has nearly attained open sea values and the suspended sediment concentrations are near those of the Gulf of St. Lawrence of about 1 mg/L.

By far the highest suspended sediment concentrations (~500 mg/L) and associated horizontal transports are evident in Figure 2 at station 6E100 which is located slightly upstream of the turbidity maximum. With only two sampling depths it is difficult to construct a complete picture but it does appear that peak concentrations follow maximum ebb and flood currents

at the lower level but that concentrations tend to be lowest during or just following the flood slack water. This suggests that vertical mixing is reduced on the flood thus inhibiting the vertical flux of suspended sediment. At this location the sediment transport is mainly in the longitudinal vertical plane as the transverse sediment flux is weak compared to the longitudinal flux.

At a station within the zone of elevated suspended sediment concentrations, but downstream of the maximum, lower concentrations allowed additional transmissometer data to supplement the centrifuge samples. It is evident that at station 6E300 in Figure 3 the mid-depth maximum in suspended sediment concentration observed further downstream by d'Anglejan and Ingram (1976) is not present. They interpreted this maximum as an indication that horizontal advection rather than local resuspension controls the sediment profiles. With the augmented data the pattern of sediment concentration fluctuation is more clear at 6E300 than at 6E100. Surface concentrations are maximum during the ebb at times of minimum vertical stratification whereas bottom concentrations peak twice a tidal cycle following maximum flow speeds. It is notable that flow reduction near the bottom causes the sediment flux to be highest at approximately two thirds of the depth. The

cross-channel component of the sediment is proportionally larger than at station 6E100.

The asymmetries in suspended sediment concentration over a tidal cycle are similar at this station to those of salt (Hamblin 1986), in that they result in an upstream Reynolds flux which closely balances the downstream advective component. Figure 4 shows the concentration profile of suspended sediment averaged over two tidal cycles based on the hourly profiles of suspended sediment from the optical transmissometer. Secondly we have that the tidally averaged advective flux, $\overline{U}\ \overline{SS}$, is downstream except for one point near the bottom whereas the residual sediment flux is weakly downstream at the surface but more strongly upstream in the lower half of the profile. The vertically averaged sediment flux is probably indistinguishable from zero at a downstream value of 0.26 g/m^2 s. Thus, it is concluded that the turbidity maximum at this station is not maintained by the gravitational circulation mechanism as described by Festa and Hansen, (1978). Since this mechanism does not seem to hold in the present data, profiles of residual along-channel currents from the data of Muir (1979) (Figure 5) show that while the classical estuarine circulation is found along the deep channel of the northwestern shoreline it does not always occur in mid channel

or along the southern shore. Residual currents in these regions are sensitive to the phase of the fortnightly tidal cycle. An in-depth examination of the origins of the tidal asymmetries in suspended sediment concentration responsible for the upstream Reynolds flux follows.

Ebb-flood asymmetry at slack water

In Figure 6, the components of bottom stress along the channel are plotted based on bottom currents measured at 30-minute intervals and the standard hydrodynamic stress law employing the drag coefficient of 1.0×10^{-3} recommended by Dewey and Crawford (1988) from the dissipation rate method. The asymmetry of the peak bottom stress between ebb and flood as suggested by Krank (1979) is not evident but rather there is asymmetry about the time of occurrence of slack water. This type of ebb-flood asymmetry has been examined in detail by Dronkers (1986) who points out that since the flow reverses more quickly as it goes from ebb to flood than from flood to ebb, there will be more material remaining in suspension during the flood cycle than in the ebb cycle. Thus there is a net landward transport of suspended sediment at the bottom.

From the viewpoint of tidal analysis the slack water asymmetry observed in this study and the peak ebb-flood asymmetry reported by Krank (1979) may be explained by overtides. The current meter data from the moorings of Budgell and Muir (1975) and Muir (1979) of the lower portion of the Upper Estuary show that, in most cases, the dominant overtide is the M4 tidal constituent (period 6.2 hr). In moorings where several current meters were established in a line the data of Budgell and Muir show that the M4 increases relatively to the predominant M2 constituent in the lower current meters and that in the case of meter 77-07C-10A080 (Muir, 1979) at a depth of 80 m and 1.5 m above the bottom the amplitude of the M4 is 22% of the M2 constituent compared to 5.4% at a depth of 10 m. The phasing of these two tidal species is not available in order to calculate whether the M4 constituent would produce the correct asymmetry for landward transport.

As well as the slack water asymmetry clearly evident in Figure 6, further landward transport may be caused by fluctuations in the vertical transport due to temporal variations in turbulent mixing. A one-dimensional model ought to be able to provide insight into this process. Additionally, it may be noted in Figure 6 that allowing for some lag the suspended sediment concentration rises, in general, when the magnitude

of the bottom stress exceeds 0.12 Pa and falls when it is less than this value. This observation will be incorporated into the simulation model to be outlined below.

Model of vertical transport of suspended sediment

The finding that local resuspension of sediments over a tidal cycle is an important process in the Upper Estuary and the need for further understanding of the residual upstream diffusive flux of sediment have led to the development of a one-dimensional mathematical model of the vertical transport of sediment. The vertical transport model for fine-grained newly-deposited sediments is described by Teeter (1986) as follows. In the case where horizontal processes are less important than vertical processes, the conservation equation for suspended sediment is (ignoring vertical advection):

$$\frac{\partial C}{\partial t} - W_s \frac{\partial C}{\partial Z} = \frac{\partial}{\partial Z}\left(K_z \frac{\partial C}{\partial Z}\right) \qquad (1)$$

where C is the concentration of the suspended sediment which varies over the vertical co-ordinate, Z, and with time t. W_s is the unknown settling velocity and the vertical eddy diffusivity, K_z is given by Fischer et al. (1979):

$$K_z = k\, u^*Z\, (h - Z)/h\, (1 + 3.33\, Ri)^{-1.5}$$

where k is the von Karman constant, 0.4, u^* is the friction velocity of the bottom boundary layer and is given by $u^* = 1 \times 10^{-3}\ U_b$ (U_b is the bottom current speed), h is the depth of the water, Ri is the Richardson number

$$Ri = g \frac{\partial \rho}{\partial Z} / \left[\left(\frac{\partial U}{\partial Z} \right)^2 + \left(\frac{\partial V}{\partial Z} \right)^2 \right]$$

where g is the acceleration of gravity and the density, ρ of the water is a function of the measured temperature, salinity and suspended sediment concentration. Measured values of the flow field and density structure are required to evaluate K_z. The observed distribution of K_z and a highly smoothed version are shown in Figure 7. The extreme variability of this quantity is related to the variation of the bottom current, Figure 6, and to the stabilizing effect on the mixing by the salt wedge during the flood. These two effects reinforce on the slack following the flood tide to produce mixing coefficients of the order of 10^{-6} m^2/s whereas during the ebb diffusivities are in the order 10^{-2} m^2/s.

Boundary conditions at the surface, Z = h, are no flux of sediment through the surface:

$$W_s C + K_Z \frac{\partial C}{\partial Z} = 0$$

and at the bottom Z = 0 there are three possible conditions;

(1) Free settling, $K_z \frac{\partial C}{\partial Z} = 0, \quad \rho u^{*2} < 0.12$ Pa

(2) Equilibrium (no flux), $W_s C + K_z \frac{\partial C}{\partial Z} = 0, \quad \rho u^{*2} \simeq 0.12$ Pa

(3) Erosion, $W_s C + K_z \frac{\partial C}{\partial Z} = -e. \quad \rho u^{*2} > 0.12$ Pa

From Figure 6 condition (1) occurs when the bottom stress is less than 0.12 Pa, condition (2) when it has a value of 0.12 Pa and (3) when the stress is greater than 0.12 Pa. The erosion rate, e, is assumed to be given by 9×10^{-5} $(U_b - 35)^2$ g/(m^2 s) based upon the discussion of Teeter (1986) and some initial sensitivity tests. The threshold bottom speed, 35 cm/s, in the above expression corresponds to a bottom stress of 0.12 Pa. The above model was solved by discretization of depth into 40 vertical grid points and an explicit

integration of the advection diffusion equation (1). Flux boundary conditions were tested with a known analytical solution and finally the sediment settling experiments of Dhamotharan et al. (1981) were duplicated by the numerical model. In the application of the model to tidal flows the initial conditions were assumed to be zero and the model was run until the concentrations were periodic over a tidal cycle (10 to 12 tidal cycles). The unknown vertical settling velocity was assumed to be constant and was determined to be 3.0×10^{-4} m/s on the basis of the best visual agreement between the observations and the model output.

Results and Discussion

The observed time histories of the vertical distribution of the suspended sediment concentration at Station 6E300 are compared to the computed distribution for the smoothed diffusivity in Figure 8 and in Figure 9 for the unsmoothed distribution. The smoothed results illustrate somewhat more clearly the influence of vertical mixing on the horizontal landward transport of sediment in the lower layers. Since the bottom current is symmetrical there are two equal pulses of high turbidity at the bottom each tidal cycle, but due to the

reduced upwards transport by the small diffusivities of the flood, more suspended sediment is retained in the lower layers and less in the upper layers than on the ebb. This explains why there is only one maximum and minimum per tidal cycle at the surface but two at the bottom. The net effect is to transport sediment landward in the lower layer particularly around 10 to 12 m in depth. In the interpretation of Figure 8 the data of Hamblin (1986) indicated that slack water occurs about one-half an hour earlier at the bottom than at the surface.

The solution based on unsmoothed diffusivities (Figure 9) demonstrates that higher bottom concentrations during low water slack are in better agreement with the field observations of Figure 8a than the solutions for the smoothed diffusivities. This is due, in part, to the slack water asymmetry described earlier.

It is perhaps fortuitous that the transmissometer failed to operate at station 6E100. Flocculation effects due to much higher concentrations of suspended sediment at that location may rule out the simplifying assumption of constant vertical settling velocity. In this case, the model would have to be enhanced along the lines discussed by Mehta (1989). The fact

that the main features of the temporal behaviour of the suspended sediment distribution can be simulated without knowledge of vertical and horizontal advection fields means that advection is less important than vertical mixing and resuspension. Employing a vertical model, Beach and Sternberg (1988) found similarly that vertical processes dominated the sediment transport in the surf zone.

Although the main use of such a model is as an aid to understanding the vertical processes responsible for sediment transport, once it is reasonably well calibrated it is possible to infer additional information which may be of application to the chemistry of contaminants even though horizontal processes are ignored. For example, the vertical flux of suspended sediment over the tidal cycle may be estimated at any level. Two levels of particular interest are mid-depth where the exchange with the seaward moving volume takes place and the bottom where the recycling with the landward displacing phase occurs. Figure 10 shows that the mid-depth flux is in phase with the bottom flux and is about one-half of the bottom flux. The instantaneous vertical sediment flux at the bottom is at least 1000 times less than the horizontal flux of suspended matter as seen in Figure 3.

From the magnitude of the vertical flux an approximate residence time for particles in suspension may be estimated. The residence time based on a vertically and tidally averaged concentration of 35 mg/L and a water depth of 25 m is 10 hours. This may be compared to the vertical advection time scale or settling time of a particle starting from the surface of 23 hours. Finally the vertical settling velocity of 3.0×10^{-4} m/s may be related to a mean particle size through the Stokes law relation which gives a size of 15 μm. This size corresponds closely to the average particle size in the turbidity maximum of 10 to 20 μm (Krank, 1979).

It is of some interest to construct a simple two-box model of suspended sediment based on exchanges between the boxes established by the continuous vertical transport model. This generalization of the data at 6E300 as shown in Figure 11 may be useful in accounting for the contaminant chemistry.

Conclusions

While there has been considerable work on the hydrodynamics and physical oceanography of the Upper St. Lawrence Estuary the current knowledge of the dynamics of sediment transport is

less satisfactory. Despite the complexity of this estuary it is shown in this study that a simple one-dimensional sediment transport model is capable of accounting for the major features of the temporal and depth behaviour provided simultaneous flow and density fields are known.

Future studies in the Upper St. Lawrence Estuary should be aimed at profiles of high speed and well-resolved suspended sediment concentrations in the region of peak turbidities where sediment flocculation effects may be important. Concurrent in situ measurements of particle settling velocities and sizes would be useful ancilliary data. Microstructure measurements of turbulent intensity and dissipation could offer much needed confirmation of the vertical eddy diffusion formula employed herein. It would be of value to estimate the contribution to the sediment conservation equation from the advection terms which have been ignored in this study. Finally, laboratory studies could provide independent information on the critical shear stress required for erosion in the model.

Acknowledgements

The loan of the conductivity-depth profiler by E. Marles is gratefully acknowledged as well as the assistance of J. Bull in translating the data tapes. Field support of P. Healey, K. Brown and C. Fergusson as well as the officers and crew of the CS Limnos contributed substantially to the success of the data collection. M. Comba is thanked for providing suspended sediment concentrations during the transmission profiles. L.R. Muir kindly permitted access to his unpublished data files of current meter observations. K.R. Lum is thanked for making possible the author's participation in the cruise on the St. Lawrence.

REFERENCES

d'Anglejan, B. and E.C. Smith. 1973. Distribution, transport and composition of suspended matter in the St. Lawrence Estuary. Can. J. Earth Sci., 10: 1380-1396.

d'Anglejan, B. and R.G. Ingram. 1976. Time-depth variation in tidal flux of suspended matter in the St. Lawrence estuary. Estuarine and Coastal Marine Sciences, 4: 401-416.

d'Anglejan, B. 1981. On the advection of turbidity in the Saint Lawrence Middle Estuary. Estuaries, 4: 2-15.

d'Anglejan, B. and R.G. Ingram. 1984. Near bottom variations of turbidity in the St. Lawrence Estuary. Estuarine, Coastal and Shelf Science, 19: 655-672.

Beach, R.A. and R.W. Sternberg. 1988. Suspended sediment transport in the surf zone: response to cross-shore infra-gravity motion. Marine Geol., 80: 61-70.

Bewers, J.M. and P.A. Yeats. 1979. The behaviour of trace metals in estuaries of the St. Lawrence Basin. Naturalist Can., 108: 149-161.

Budgell, W.P. and L.R. Muir. 1975. St. Lawrence River Current Survey 1974 Data Report. Ocean and Aquatic Sciences Dept. of Environment, Burlington. Unpublished report.

Cossa, D. and S.A. Poulet. 1978. Survey of trace metal contents of suspended matter in the St. Lawrence Estuary and Saguenay Fjord. J. Fish Res. Board Can., 35: 338-345.

Dewey, R.D. and W.R. Crawford. 1988. Bottom stress estimates from vertical dissipation rate profiles on the continental shelf. J. Phys. Oceanogr., 18: 1167-1177.

Dhamotharan, S., Gulliver, J.S. and Stefan, H.G. 1981. Unsteady one-dimensional settling of suspended sediment. Water Res., 17: 1125-1132.

Dronkers, J. 1986. Tide-induced residual transport of fine sediment. In Physics of Shallow Estuaries and Bays. Ed. J. Van De Kreeke. Springer-Verlag, pp. 228-244.

El-Sabh, M.I. 1988. Physical Oceanography of the St. Lawrence Estuary. In Hydrodynamics of Estuaries, Vol II, Estuarine Case Studies, CRC Press, pp. 61-78.

Festa, J.F. and D.V. Hansen. 1978. Turbidity maximum in partially mixed estuaries: a two dimensional numerical model. Estuarine and Coastal Marine Science, 7: 347-359.

Fischer, H.B., E.J. List, R.C.Y. Koh, J. Imberger and N.H. Brooks. 1979. Mixing in inland and coastal waters. Academic Press.

Hamblin, P.F. 1986. Upper St. Lawrence Estuary Circulation Study, 1986: Preliminary Analysis and Data Report. National Water Research Institute Report No. 87-83.

Krank, K. 1979. Dynamics and distribution of suspended particulate matter in the St. Lawrence Estuary. Le Naturalist Can., 106: 163-173.

Mehta, A.J. 1989. Cohesive sediments in estuarine environment. In Press, J. Geophy Res-Oceans.

Muir, L.R. 1979. St. Lawrence River oceanographic survey. 1977. Data Report Vol. 1, Tidal, Meterological and Current Meter Data. Data Report Series 79-1, Fisheries and Oceans.

Nichols, M.N. 1986. Effects of fine sediment resuspension in estuaries. In Estuarine Cohesive Sediment Dynamics. Ed. A.J. Mehta. Springer-Verlag, pp. 5-42.

Silverberg, N. and B. Sundby. 1979. Observations in the turbidity maximum of the St. Lawrence Estuary. Can. J. Earth Sci., 16: 939-950.

Soucy, A.Y., Y. Berubé, J.P. Fronder and P. Merie. 1976. Évolution des suspensions et sediments dans l'estuarie moyen du Saint Laurent. Le Cahier de Centreau, 1(5): 67.

Teeter, A. 1986. Vertical transport in fine-grained suspended and newly deposited sediment. In Estuarine Cohesive Sediment Dynamics, Ed. A.J. Mehta. Springer Verlag, pp. 170-191.

FIGURES

Figure 1 Study location and simplified bathymetry of Upper St. Lawrence Estuary.

Figure 2 Time-depth distributions at station 6E100 of (a) suspended sediment concentration, (b) horizontal sediment flux, and (c) salinity (g/L). The longitudinal reference axis is taken as positive in the seaward direction.

Figure 3 Same as Figure 2 except at 6E300.

Figure 4 Tidally-averaged suspended sediment, $\overline{SS}$, product residual along-channel flow, $\overline{U}$, and $\overline{SS}$ and longitudinal Reynolds sediment transport, $\overline{U'SS'}$ at station 6E300. Primed quantities are deviations from the tidal average denoted by overbar.

Figure 5 Along-channel tidal residual current Pointe-au-Pic, 1975, profiles measured at different times at a station are plotted along the axis of the channel. Sp=spring tides, NP=neap tides.

Figure 6 Suspended sediment concentration at bottom, -----. Along-channel component of bottom stress, Pa,_____. Station 6E300.

Figure 7 Time history over the water column of the vertical eddy diffusivity at station 6E300 (m^2/s) over a tidal cycle. (a) Unsmoothed, (b) smoothed. E is ebb; S is slack and F is flood.

Figure 8 Time history of suspended sediment concentration at Station 6E300 (mg/L), (a) observations based on transmissometer profiles, (b) simulated with smoothed diffusivity.

Figure 9 Same as Figure 8(b) but simulated with unsmoothed diffusivities.

Figure 10 Upward vertical flux of suspended sediment $mg/(m^2/s)$ at (a) mid-depth, (b) bottom, over the tidal cycle predicted from vertical transport model.

Figure 11 Two-box model of suspended sediment, C, and salinity, S, and associated horizontal and vertical exchanges at Station 6E300.

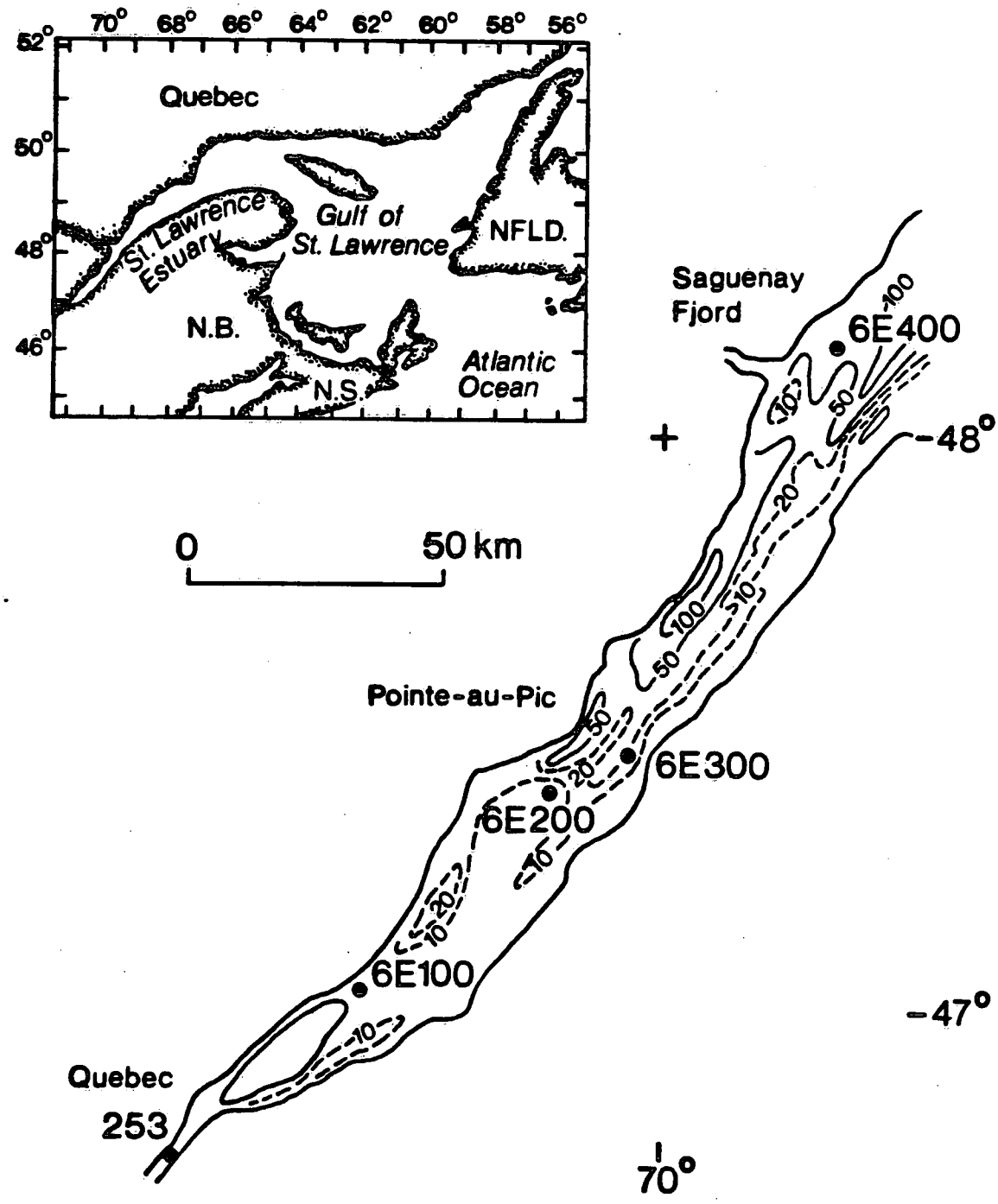
70° 68° 66° 64° 62° 60° 58° 56°
52°
50°
48°
46°
Quebec
St. Lawrence Estuary
Gulf of St. Lawrence
NFLD.
N.B.
N.S.
Atlantic Ocean
0
50 km
Saguenay Fjord
6E400
-48°
Pointe-au-Pic
6E300
6E200
6E100
-47°
Quebec
253
70°
100
50
30
20
10

Figure 1

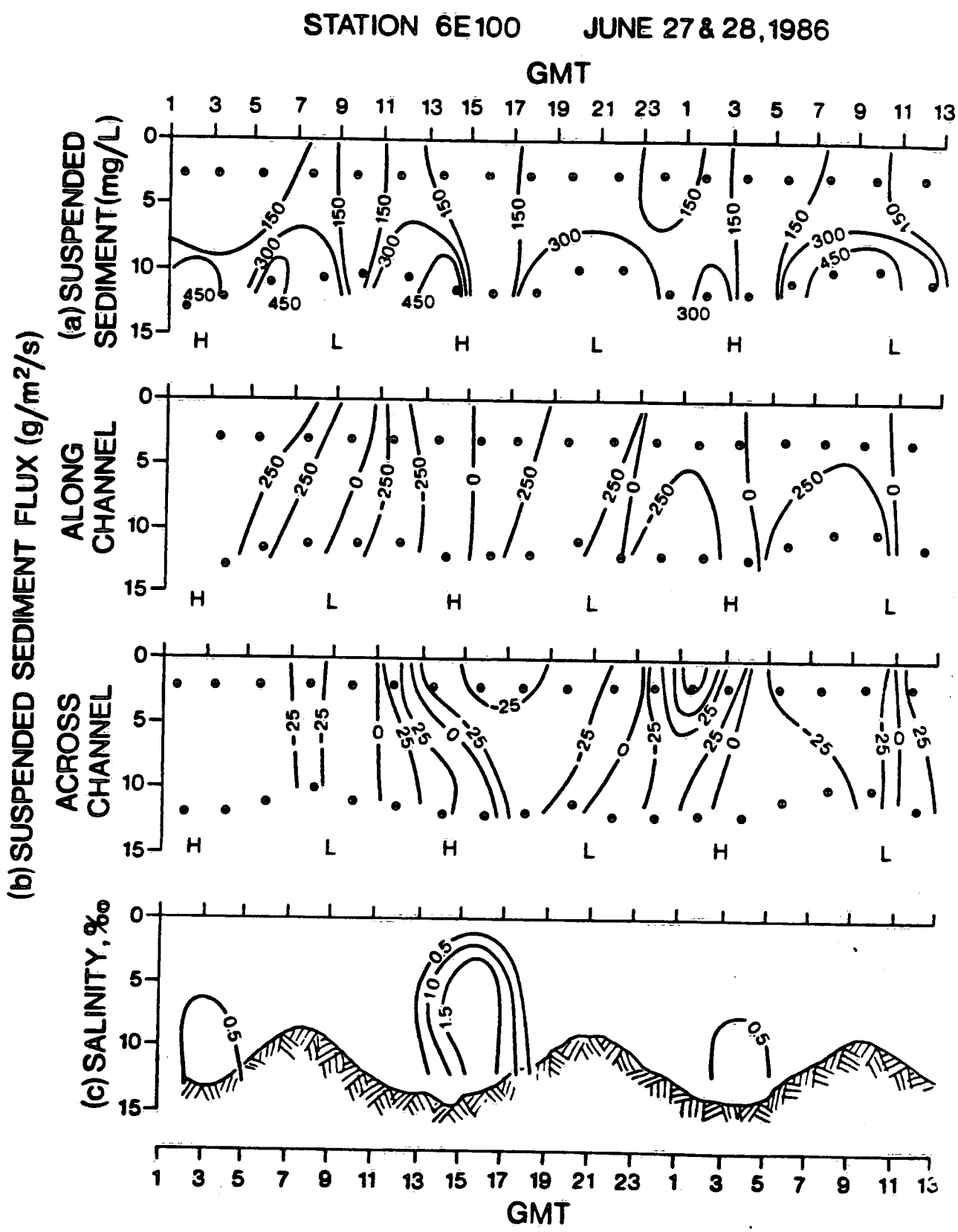
STATION 6E100 JUNE 27 & 28, 1986
GMT
(a) SUSPENDED SEDIMENT (mg/L)
(b) SUSPENDED SEDIMENT FLUX (g/m²/s)
ALONG CHANNEL
ACROSS CHANNEL
(c) SALINITY, ‰
H
L
GMT

Figure 2

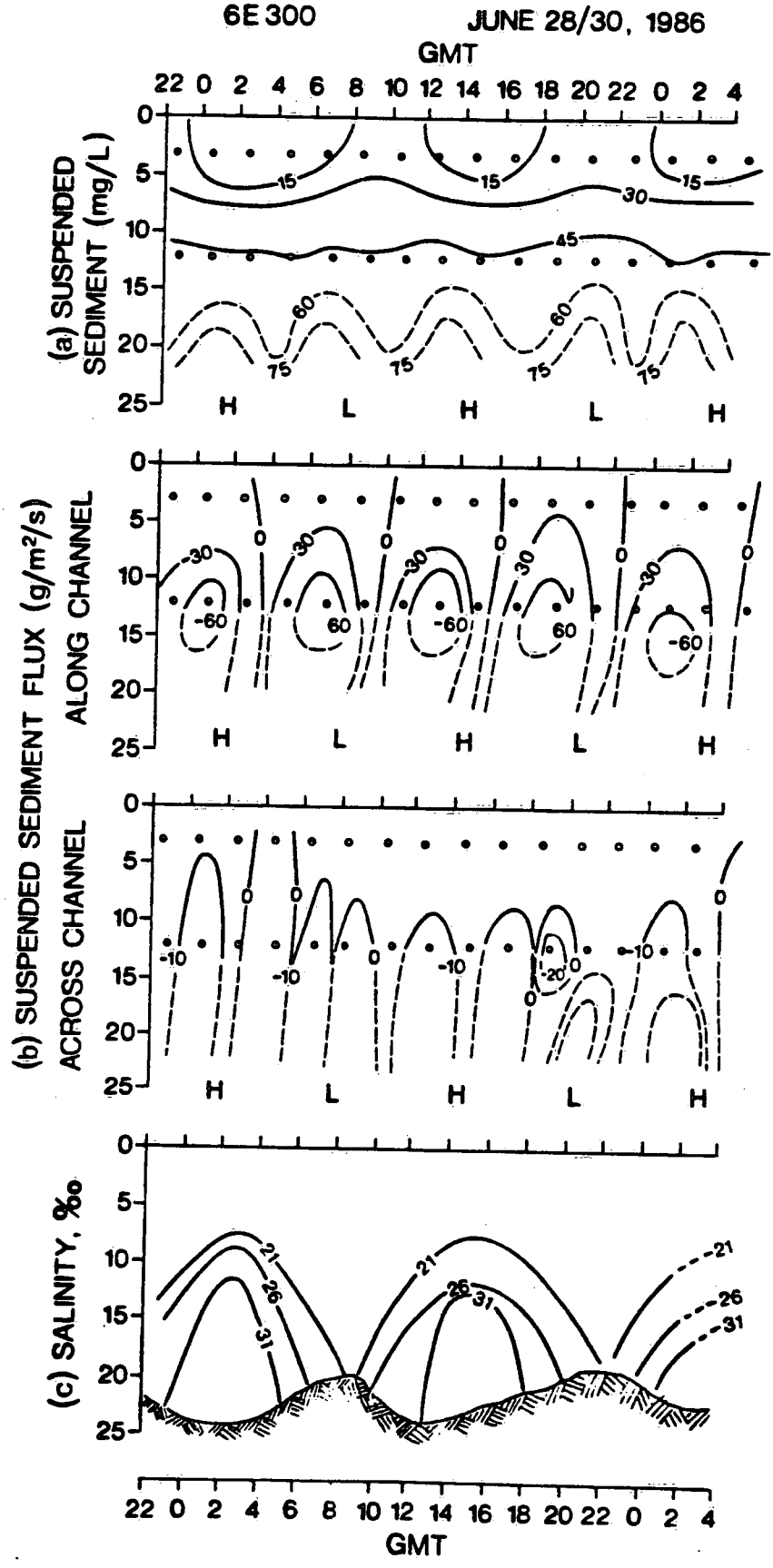
6E 300
JUNE 28/30, 1986
GMT
22 0 2 4 6 8 10 12 14 16 18 20 22 0 2 4
(a) SUSPENDED SEDIMENT (mg/L)
15
30
45
60
75
H L H L H
(b) SUSPENDED SEDIMENT FLUX (g/m²/s)
ALONG CHANNEL
ACROSS CHANNEL
-30
-60
-10
-20
(c) SALINITY, ‰
21
26
31
0 5 10 15 20 25

Figure 3

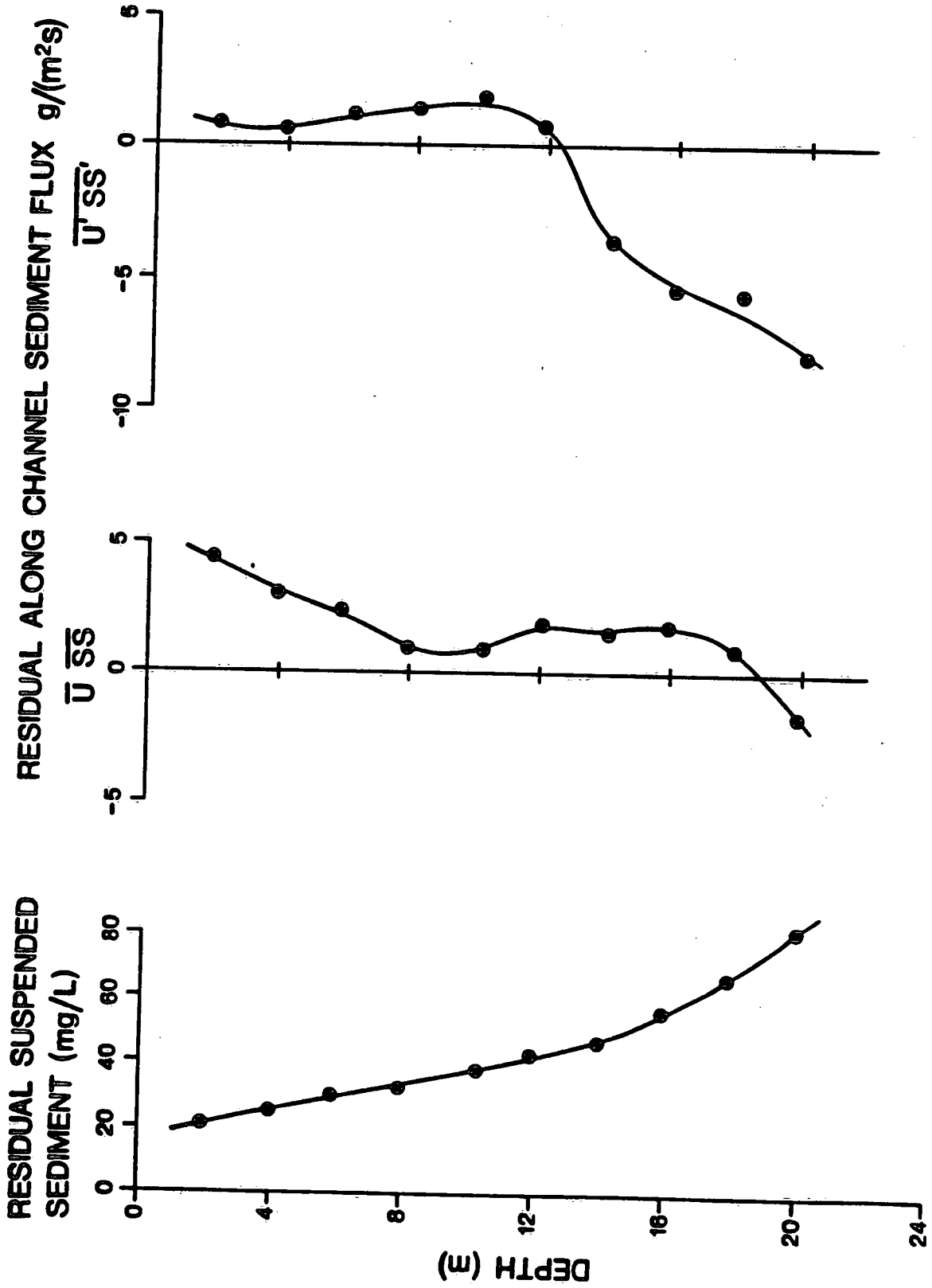
RESIDUAL SUSPENDED SEDIMENT (mg/L)
0
20
40
60
80
RESIDUAL ALONG CHANNEL SEDIMENT FLUX g/(m²s)
$\overline{U}\,\overline{SS}$
5
0
-5
$\overline{U'SS'}$
5
0
-5
-10
DEPTH (m)
0
4
8
12
16
20
24

Figure 4

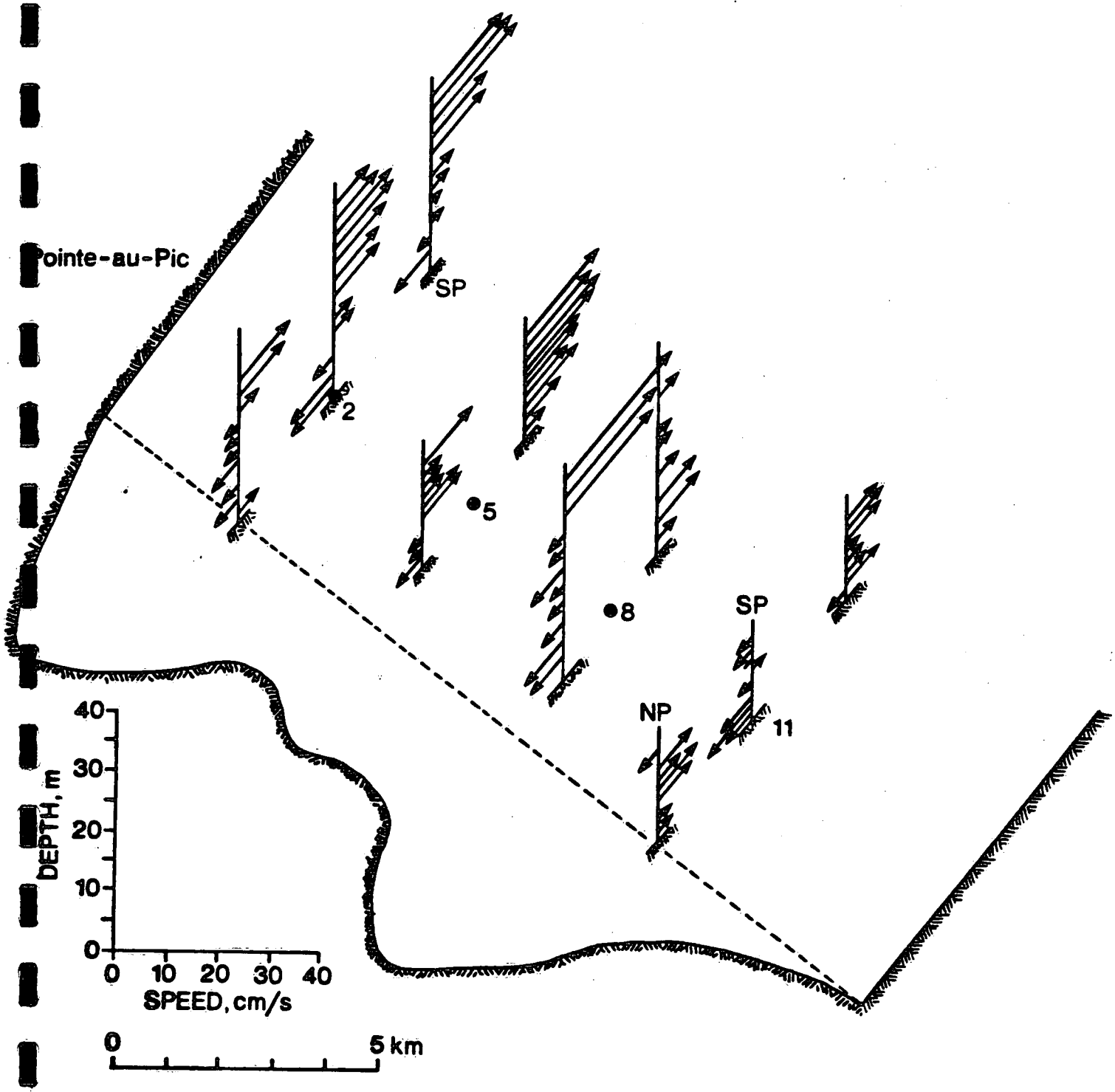
Pointe-au-Pic
SP
2
5
8
SP
NP
11
40
30
20
10
0
DEPTH, m
0 10 20 30 40
SPEED, cm/s
0
5 km

Figure 5

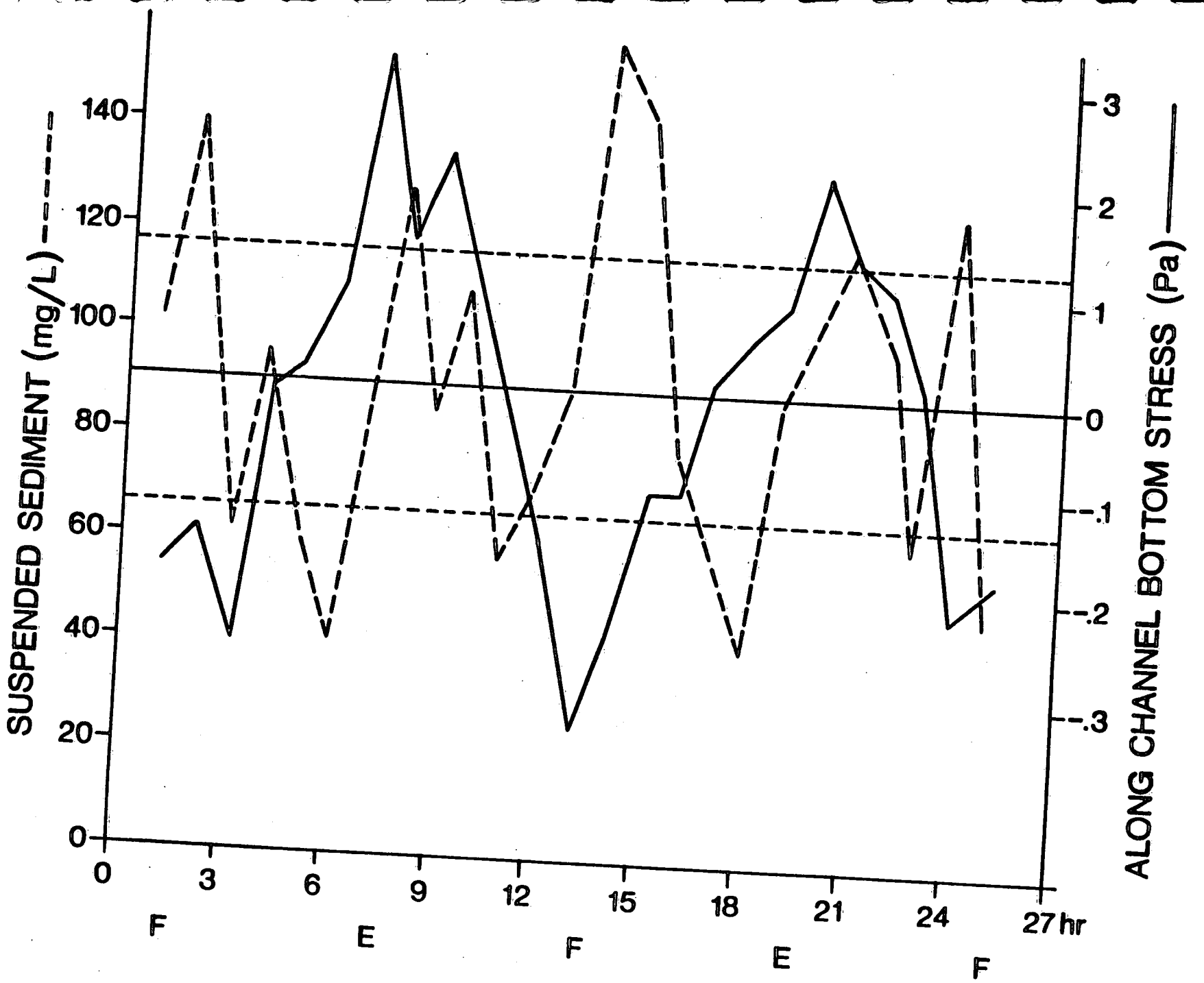
SUSPENDED SEDIMENT (mg/L)
ALONG CHANNEL BOTTOM STRESS (Pa)
140
120
100
80
60
40
20
0
3
2
1
0
.1
.2
.3
0
3
6
9
12
15
18
21
24
27 hr
F
E
F
E
F

Figure 6

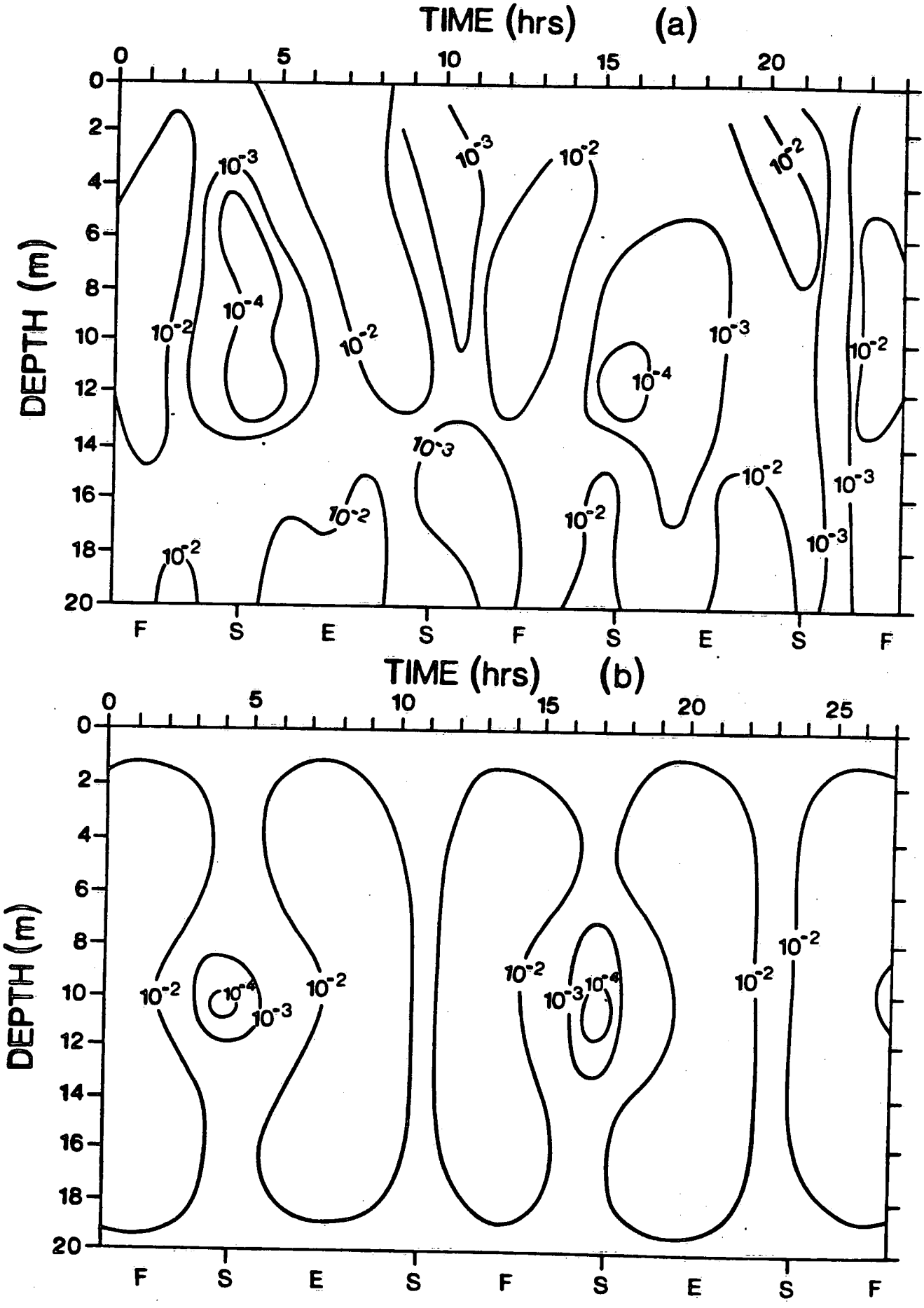
TIME (hrs) (a)
DEPTH (m)
0
5
10
15
20
2
4
6
8
10
12
14
16
18
10^{-2}
10^{-3}
10^{-4}
F
S
E
S
F
S
E
S
F
TIME (hrs) (b)
DEPTH (m)
0
5
10
15
20
25
2
4
6
8
10
12
14
16
18
20
10^{-2}
10^{-3}
10^{-4}
F
S
E
S
F
S
E
S
F

Figure 7

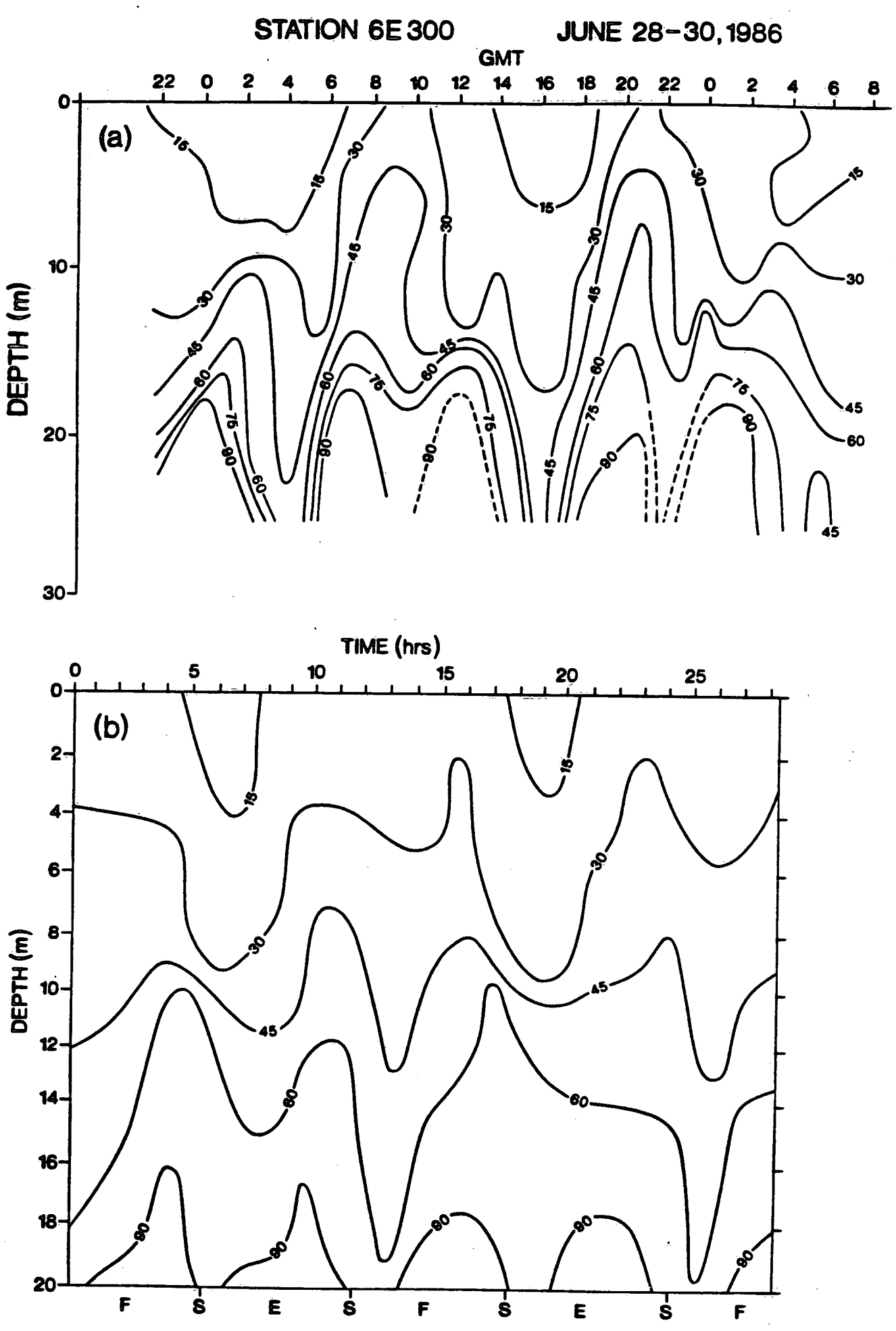
STATION 6E300
JUNE 28-30, 1986
GMT
22 0 2 4 6 8 10 12 14 16 18 20 22 0 2 4 6 8
(a)
DEPTH (m)
0
10
20
30
15
30
45
60
75
90
(b)
TIME (hrs)
0 5 10 15 20 25
DEPTH (m)
0 2 4 6 8 10 12 14 16 18 20
F S E S F S E S F

Figure 8

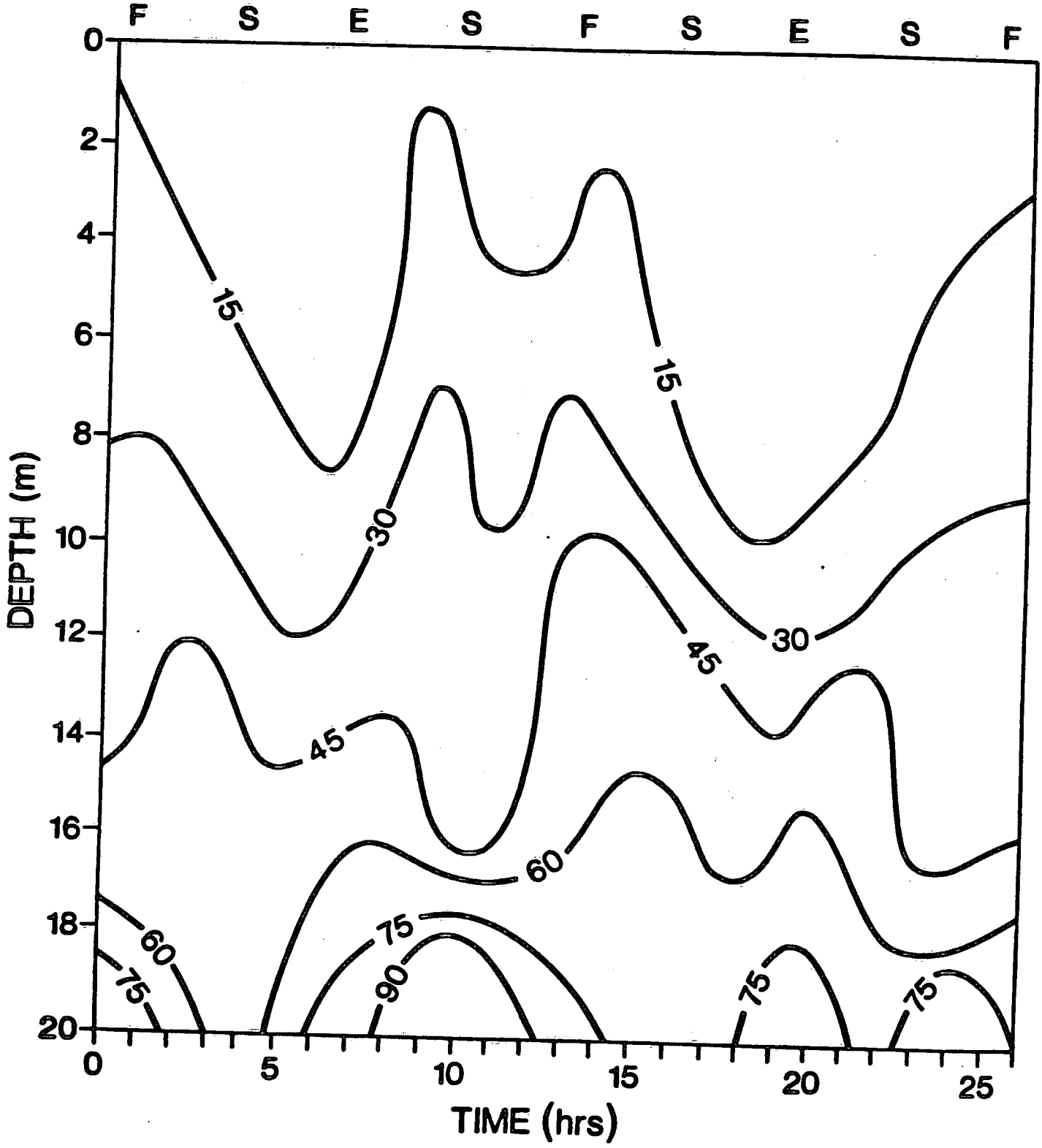
F
S
E
S
F
S
E
S
F
0
2
4
6
8
10
12
14
16
18
20
DEPTH (m)
15
15
30
30
45
45
60
60
75
75
90
75
75
0
5
10
15
20
25
TIME (hrs)

Figure 9

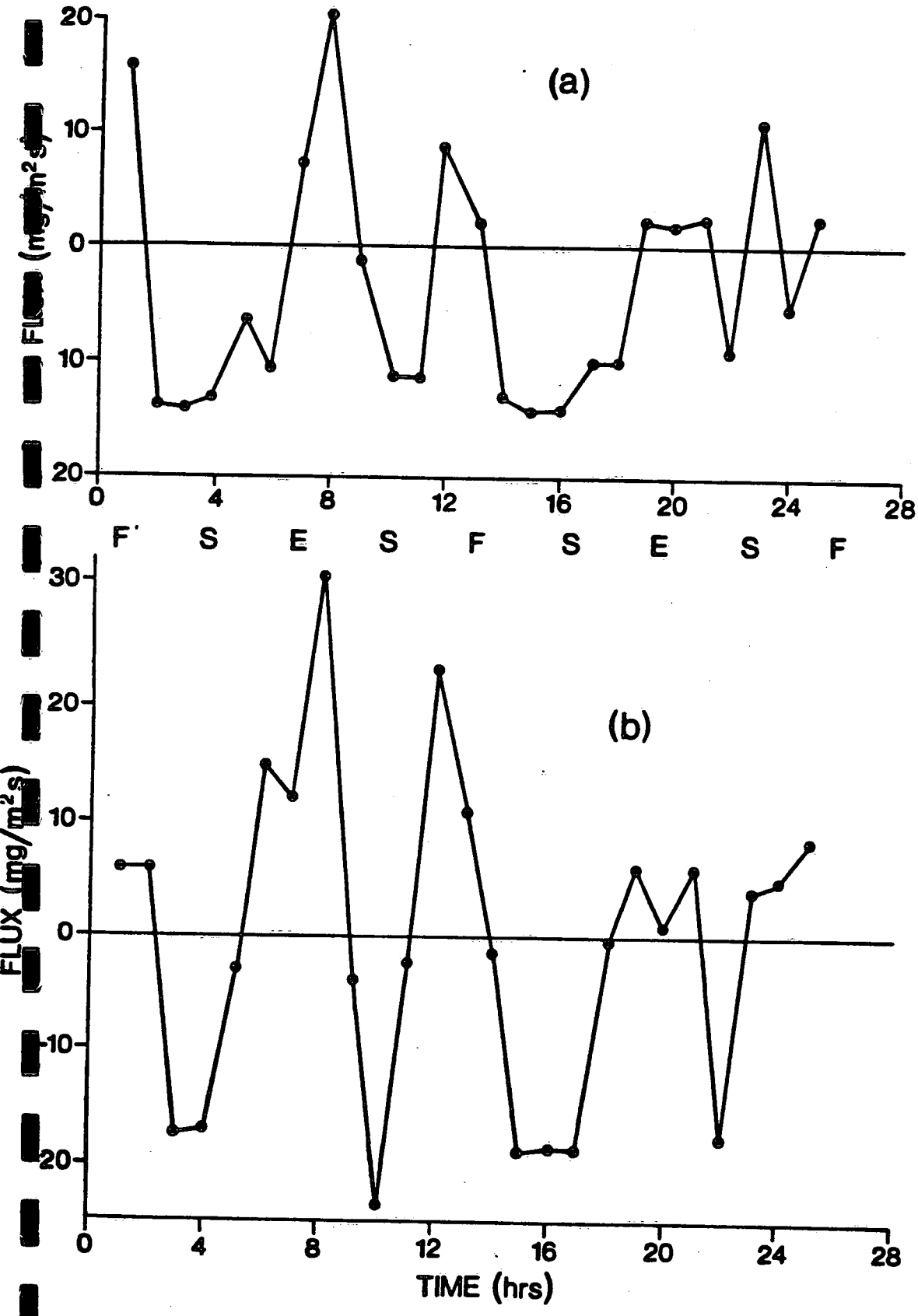
(a)
20
10
0
10
20
0
4
8
12
16
20
24
28
F S E S F S E S F
(b)
30
20
10
0
10
20
FLUX (mg/m²s)
0
4
8
12
16
20
24
28
TIME (hrs)

Figure 10

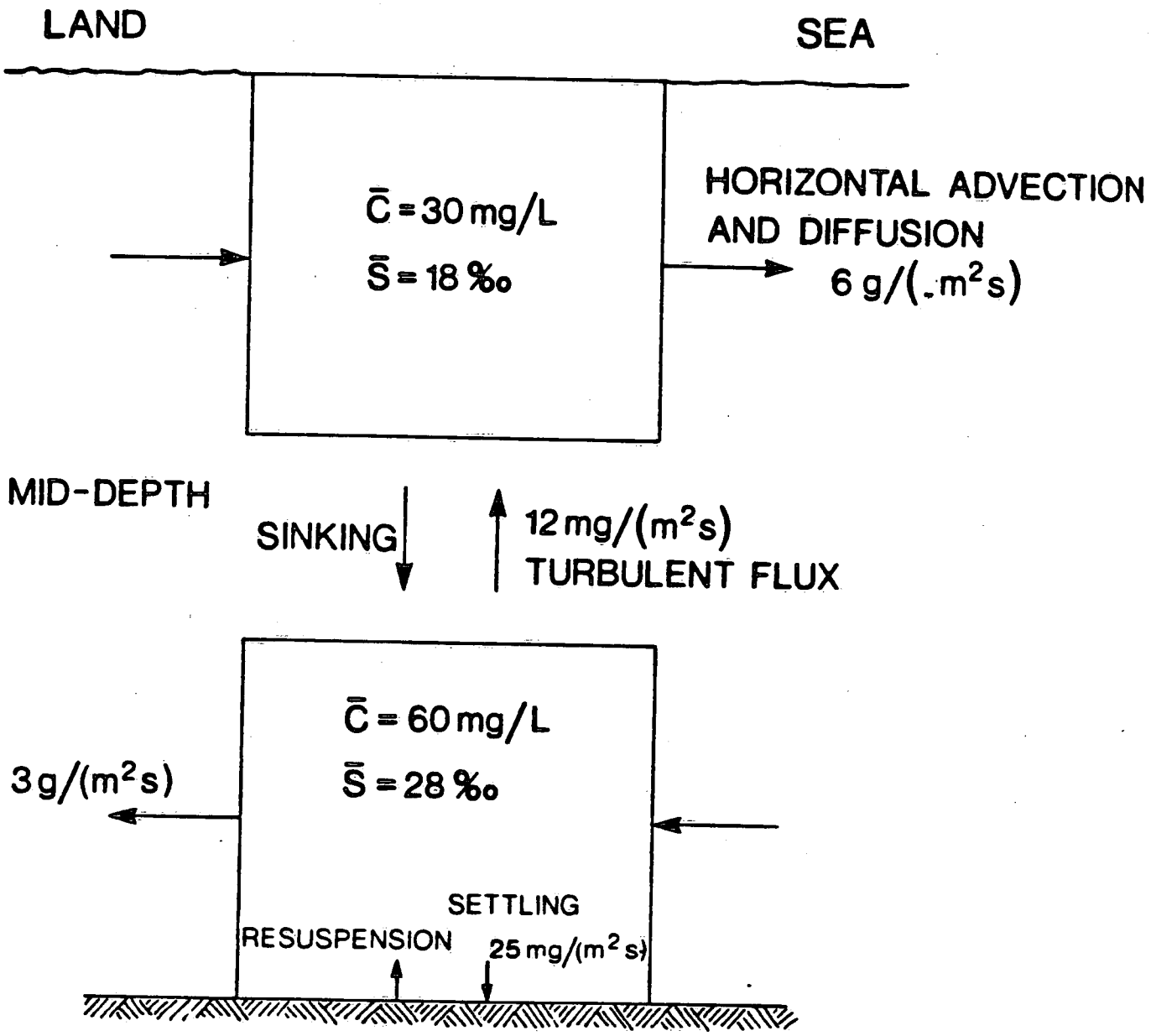
LAND
SEA
$\bar{C}$ = 30 mg/L
$\bar{S}$ = 18 ‰
HORIZONTAL ADVECTION
AND DIFFUSION
6 g/(m²s)
MID-DEPTH
SINKING
12 mg/(m²s)
TURBULENT FLUX
$\bar{C}$ = 60 mg/L
$\bar{S}$ = 28 ‰
3 g/(m²s)
SETTLING
RESUSPENSION
25 mg/(m²s)

Figure 11